

## Structural evaluation of an existing steel natatorium by FEM and dynamic measurement

Wei Liu<sup>†</sup>, Wei-Cheng Gao<sup>‡</sup>, Yi Sun<sup>††</sup> and Yan-Lei Yu<sup>‡‡</sup>

*Department of Astronautics Science and Mechanics, Harbin Institute of Technology,  
Harbin 150001, China*

*(Received June 5, 2008, Accepted February 27, 2009)*

**Abstract.** Based on numerical and experimental methods, a systematic structural evaluation of a steel natatorium in service was carried out in detail in this paper. Planning of inspection tasks was proposed firstly according to some national codes in China in order to obtain the economic and reliable results. The field visual inspections and static computation were conducted in turn under in-service environmental conditions. Further a three-dimensional finite element model was developed according to its factual geometry properties obtained from the field inspection. An analytical modal analysis was performed to provide the analytical modal properties. The field vibration tests on the natatorium were conducted and then two different system identification methods were used to obtain the dynamic characteristics of the natatorium. A good correlation was achieved in results obtained from the two system identification methods and the finite element method (FEM). The numerical and experimental results demonstrated that the main structure of the natatorium in its present status is safe and it still satisfies the demand of the national codes in China. But the roof system such as purlines and skeletons must be removed and rebuilt completely. Moreover the system identification results showed that field vibration test is sufficient to identify the reliable dynamic properties of the natatorium. The constructive suggestion on structural evaluation of the natatorium is that periodic assessment work must be maintained to ensure the natatorium's safety in the future.

**Keywords:** triangle steel tube truss; field inspection; structural evaluation; dynamic measurement; operational modal analysis.

---

### 1. Introduction

Many large civil structures such as gymnasium, bridge and offshore structures often need in-service inspection to ensure their safety, durability and operability. Adequate inspections can prevent sudden failure due to the accumulative damage or deterioration under all loading and environmental conditions. These loading conditions include seismic action, wind action, traffic action, internal pressure, prestress forces, thermal expansion and moisture expansion, etc. During the service life of civil structures the corrosion damage and fatigue damage are the main problems after some time in

---

<sup>†</sup> Ph.D., Corresponding author, E-mail: liuweiliuwei2005@gmail.com, liuweiliuwei2003@hit.edu.cn

<sup>‡</sup> Professor, E-mail: gaoweicheng@sina.com

<sup>††</sup> Professor, E-mail: sunyi@hit.edu.cn

<sup>‡‡</sup> Doctoral Candidate, E-mail: yyl\_606@yeah.net

operation. So its negative effects on the performance of the structures should be explicitly considered especially if its service life is extended. Hai (2006) explored the current status of in-service railway bridges in Vietnam and reviewed the deficiencies occurring on steel structures. The research results showed that the existing bridges are in a state of poor physical condition and have many deficiencies such as corrosion, fatigue, cracks, distress, aging, excessive deformation, premature material deterioration, functional obsolescence, and even missing elements, human invasions, etc. McCrea *et al.* (2002) concluded the corrosion damage and deterioration problems on steel bridges depending on their type and location, and identified the commonly used inspection and restoration methods. Melchers (2005) considered the essential theoretical concepts and data requirements for engineering structural reliability assessment suitable for the corroding offshore structures and pipelines. An important outcome is that good quality estimation of the structural integrity requires good modelling of the longer-term corrosion behaviour. Onoufriou *et al.* (2002) presented a brief retrospection of the development and application of reliability-based assessment techniques for the offshore and bridge structures. The similarities and differences between inspection optimizations for offshore and bridge structures are also discussed.

Accumulative damage and structural deterioration such as corrosion, fatigue, cracks, aging and excessive deformation will cause changes in the physical properties (mass, damping and stiffness) of the structure. Moreover modal parameters are functions of the physical properties of the structure and changes in the physical properties will cause changes in the modal properties. So, some work had also been done in evaluating structural performance by determining the modal properties of the structure through the full-scale vibration test (Wenzel *et al.* 2001). Field vibration test is the on-site dynamic test under the natural excitations such as traffic, winds, earthquakes and other environmental loads. The advantage of the field vibration test is that the structure can remain in its normal operating condition and the identified modal parameters can be utilized directly in vibration-based damage detection and structural health monitoring of the structures (Zhang *et al.* 2005). Therefore, field vibration tests have been successfully applied to many large-scale civil structures such as suspension bridge (Abdel 1985, Siringoringo 2008), cable-stayed bridge (Cunha 2001, Ren 2005, Galvin 2007), old multi-tiered temple (Jaishi 2003), historic masonry tower (Gentile 2007) and stadium suspended roof (Magalhaes 2008). All the results can provide reliable and accurate estimates of the modal parameters although the actual loading conditions are not measured. Further the next-step research emphases in the above papers are respectively put on damage assessment and seismic capacity evaluation.

In this paper structural evaluation of a steel natatorium in service is carried out based on the numerical and experimental methods. The objective is to present a systematic evaluation scheme on structural performance of the natatorium and perform the maintenance or restoration work to remove the existing deficiencies. The outline of the paper is as follows: Section 2 describes the structural type, structural array and physical dimension of the natatorium in detail; Section 3 presents the whole evaluation scheme on the in-service performance of the natatorium; Further the field visual inspections and static computation is conducted under an actual service environment in Section 4 and Section 5 respectively; Then the three-dimensional finite element model of the natatorium is developed according to its factual geometry properties from the field inspection and the analytical modal analysis is carried out in Section 6; Section 7 presents the whole process of the field vibration test on the natatorium. To characterize its dynamic properties two system identification methods are evaluated only using the response data in this study. They are Stochastic Subspace Identification (SSI-DATA) method (Overschee 1996), Frequency Domain Decomposition (FDD) / the Frequency-

Spatial Domain Decomposition (FSDD) method (Brincker 2001, Zhang 2005, Wang 2005). Finally the conclusions and suggestions gained in this paper are summarized in Section 8.

## 2. Description of the natatorium

The culture natatorium in National Science Park of Harbin Engineering University is constructed in the year of 2003, Heilongjiang Province, China. It is the main recreational room of the staffs and their families in National Science Park. The structural layout plan of the natatorium can be seen in Fig. 1. The main structure is the triangle steel tube truss. The span of the steel tube truss is

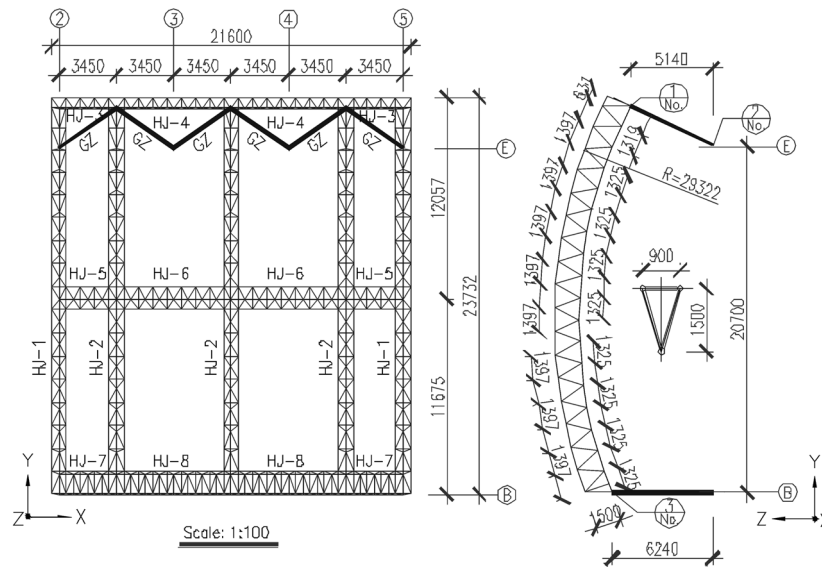


Fig. 1 Structural layout plan of the natatorium (units: mm)

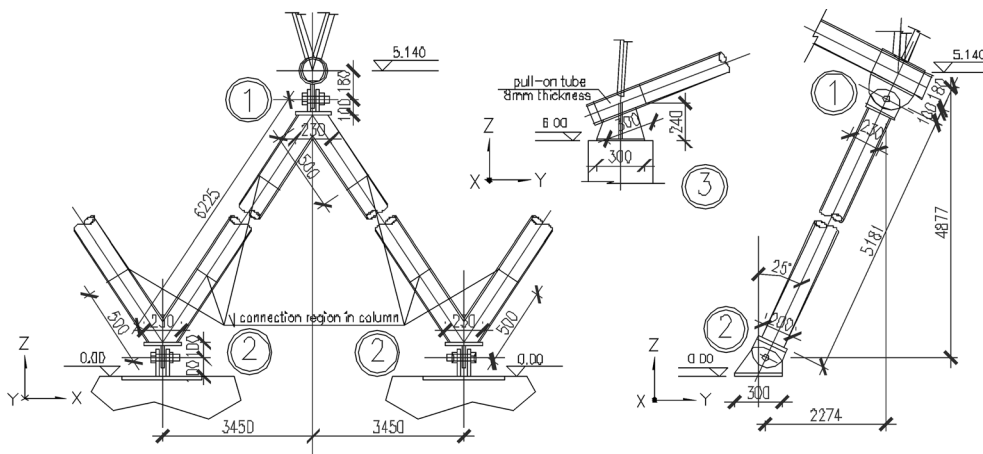


Fig. 2 The detail drawing of the connection nodes (units: mm)

23.732 m and the building area is 512.6 m<sup>2</sup>. One support of the steel tube truss (HJ-1 or HJ-2 in Fig. 1) is located on the top of the declining lambdoid steel column (GZ in Fig. 1) in ⑤ axis and another is located on the top of the concrete column in ② axis. The detail drawing of the connection nodes is shown in Fig. 2. Totally five main trusses (two HJ-1, three HJ-2) in the longitudinal direction are used and connected by three groups of connection trusses (two HJ-3 and

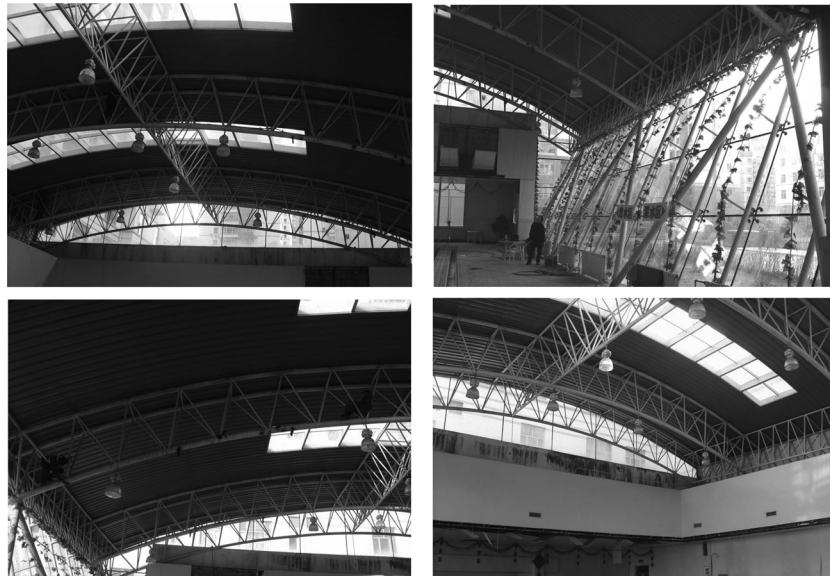


Fig. 3 View of the natatorium

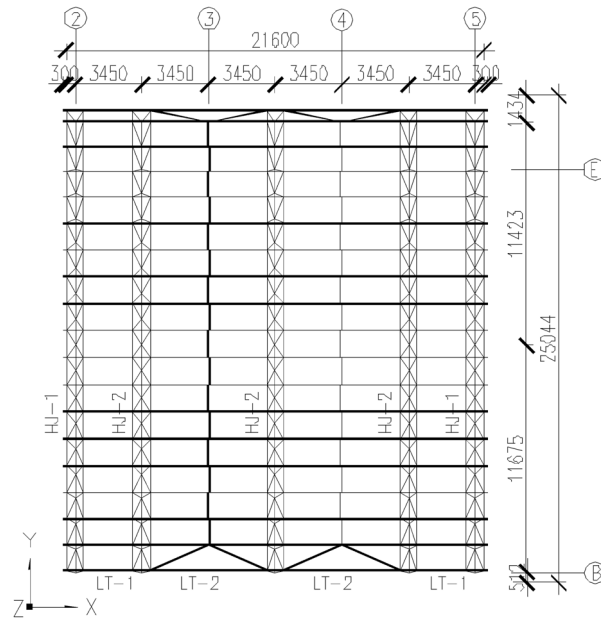


Fig. 4 Layout of the purlines (units: mm)

two HJ-4, two HJ-5 and two HJ-6, two HJ-7 and two HJ-8) in the latitudinal direction. They formed the whole spatial structure in company with the roof system and the glass curtain walls. The view of the natatorium can be seen in Fig. 3.

The nominal values of the design loads are listed as follows: permanent load is  $0.8 \text{ kN/m}^2$ , variable load is  $0.5 \text{ kN/m}^2$ , reference wind pressure is  $0.45 \text{ kN/m}^2$ . The material of the steel truss is taken as Q235BF. The section dimensions of the trusses are determined in the design process. In detail, the section dimensions of the elements in main trusses (HJ-1 and HJ-2) are  $\Phi 48 \times 3.0 \text{ mm}$ ,  $\Phi 60 \times 3.2 \text{ mm}$ ,  $\Phi 76 \times 3.75 \text{ mm}$ ,  $\Phi 108 \times 4.7 \text{ mm}$ ,  $\Phi 133 \times 4.7 \text{ mm}$  and  $\Phi 159 \times 8.0 \text{ mm}$  respectively, where the symbol ' $\Phi$ ' is the diameter of the truss member. The section dimensions of the connection trusses (HJ-3 to HJ-8) are respectively  $\Phi 48 \times 3.0 \text{ mm}$ ,  $\Phi 76 \times 3.75 \text{ mm}$  and  $\Phi 89 \times 3.75 \text{ mm}$ . The section dimension of the declining lambdoid steel column (GZ) is  $\Phi 159 \times 6.0 \text{ mm}$ . The glass curtain walls are hung using the prestressed cable-bar trusses on the outside of the declining lambdoid steel columns. The colour interlayer steel plate with the thick rock wool is adopted as the roof system. The C section steel purlines are laid snugly in one-way form and the dimension is  $C160 \times 70 \times 20 \times 3$ . The layout of the C purlines can be seen in Fig. 4 and two draw bars are designed and located in ③ axis and ④ axis respectively.

### 3. Evaluation scheme on structural performance

From 2003 to now, the steel structure natatorium has immersed in the water vapour environment with a mass of chlorine (Cl) at Celsius  $20 \sim 25$  degree all through. And the maximum difference between the indoor temperature and outdoor temperature has exceeded 60 degree Celsius. At present the steel tube trusses have already corroded from lightness to severity and the local surfaces of the trusses have developed some obvious moss. Through the visual observation the rust-eaten result of the skeleton is very serious. The cable which hung the glass curtain wall also became loose. At the same time the corrosion results of the column bases and the purlines are unclear. So it is necessary to execute the safety inspection to evaluate the structural performance of the steel natatorium. The structural evaluation contents should include inspection on the integrality of the whole structure, inspection on the component and connection, static computation of the whole structure, modal analysis by FEM and field vibration test.

After above initial observation and diagnosis the whole evaluation scheme on the structural performance of the natatorium was proposed. Planning of inspection tasks is important in order to obtain the economic and reliable results. The referenced national codes in China are listed as bellows: a) Technical standard for inspection of building structure (GB/T 50344 - 2004); b) Code for acceptance of construction quality of steel structures (GB 50205-2001); c) Standard for testing of engineering quality of glass curtain walls (JGJ/T 139-2001); d) Code for acceptance of construction quality of roof (GB 50207-2002); e) Code for design steel structures (GB 50017-2003); f) Other current relational national standards and codes. The evaluation scheme on structural performance of the natatorium is based on field inspection and theory analysis. The flow chart of the whole evaluation scheme is shown in Fig. 5.

The structural evaluation process is conducted as follows:

- (i) Conduct initial field inspection (whole structure, components and connections, loads);
- (ii) Implement inspection on static and dynamic properties of the structure (strength, stiffness, modal parameters);

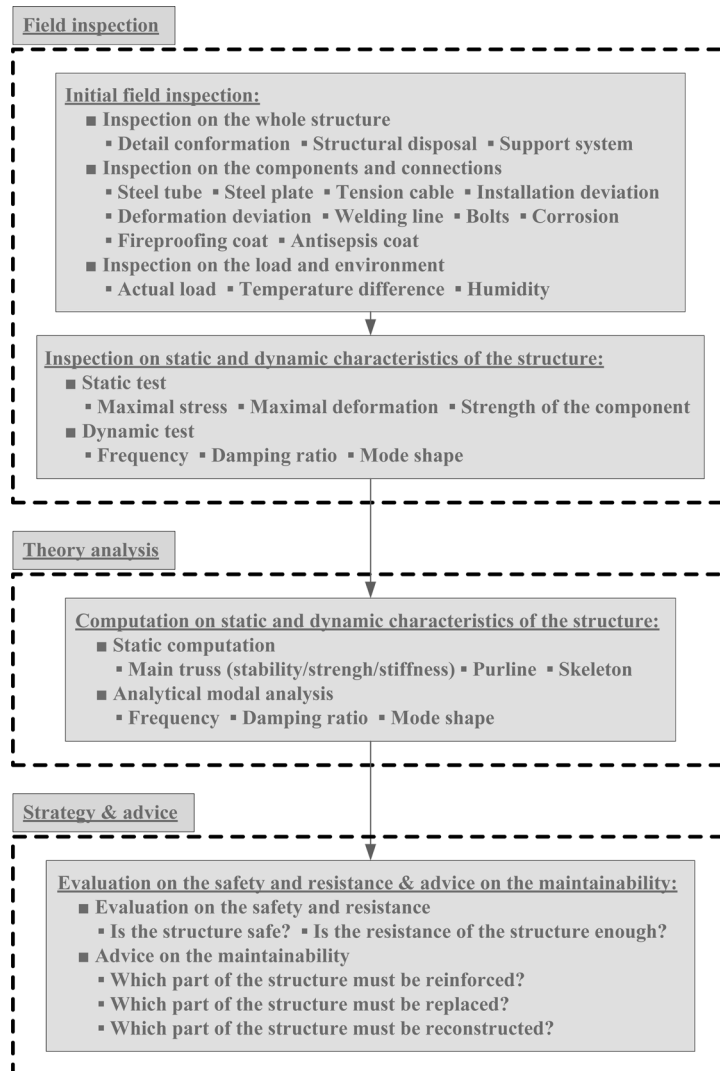
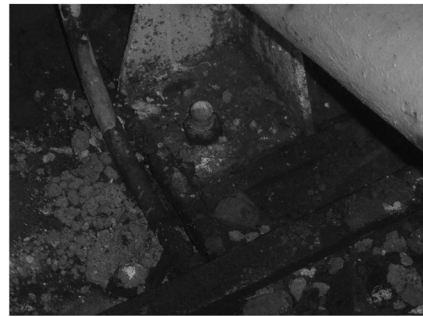


Fig. 5 Flow chart of the whole evaluation scheme

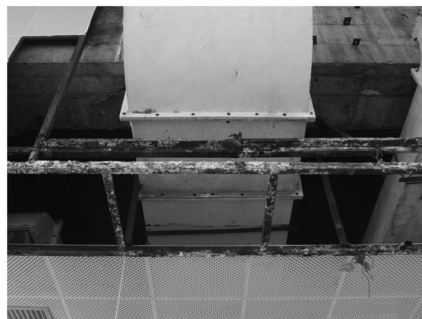
- (iii) Perform structural analysis to assess its current structural performance (static analysis, dynamic analysis);
- (iv) Present some rational advice on maintenance and update the structural performance of existing structure.

#### 4. Field inspection

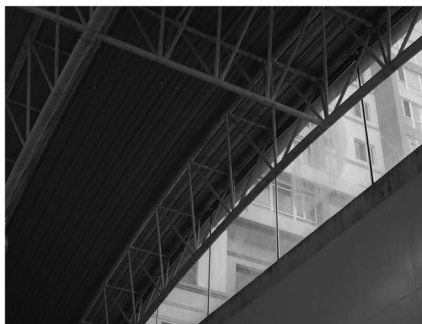
Firstly inspection on the whole structure was carried out. The results showed that the detail conformation, structural layout and support system are basically consistent with the design drawing. Secondly inspection on the components and connection was performed. After the random sampling



(a) Corrosion results of the column base



(b) Corrosion results of the skeleton



(c) Corrosion results of the steel tube truss



(d) Corrosion results of the purlines

Fig. 6 Inspection results of the corrosive structure

inspection on some components, the specification and section dimensions of the components are basically consistent with the design drawing. The components also have no obvious installation deviation and deformation deviation. Meanwhile the actual strength of the steels also satisfied the design value. Further the numbers and specifications of the bolts are also same as the design drawing's. There is no obvious weld defect and damage can be found in weld joints through the non destructive testing. One awful thing is that the top coat of the steel truss has partially sloughed.

After these secondary inspections had been completed, the emphasis was put on the inspection of the corrosion state. The corrosion is the main strength degradation phenomenon, generally accounted for as uniform corrosion wastage. Corrosion wastage increases nominal stresses and hence, induces earlier fatigue failure, as well as reduces ultimate strength capacity. And if corrosion allowance is exceeded, the component must be replaced after the field inspection. Fig. 6(a) showed the supports of the steel columns in ⑤ axis (left) and the supports on the concrete columns in ⑥ axis (right). It is obvious that the top coat has slough off badly. Fig. 6(b) showed the serious corrosion results of the skeleton, which hung on the suspended ceiling. Observing them we can see that some elements have delaminated and retreated from work thoroughly. Fig. 6(c) showed the corrosion results of the steel tube truss. Obviously the top coat of the steel tube truss has slough off. Fig. 6(d) showed the corrosion results of the purlines. The purlines have eroded and delaminated entirely because of the accumulated water on the roof. The results are very serious.

## 5. Static computation

After field inspection it is necessary to perform static computation on the whole steel structure and the purlines. Firstly the effective sections of the members after corrosion are measured and compared with the design's as shown in Table 1. Observing them we can get that the cross section

Table 1 Inspection on the effective sections of the corrosive components

Inspection item	Measure value (mm)	Design value (mm)	Corrosion rate (%)	Corrosion speed rate (mm/year)
Thickness of the base plate on the steel column (Fig. 6(a) left)	15.2	16.0	5.0	0.27
Thickness of the base plate on the concrete column (Fig. 6(a) right)	9.4	10.0	6.0	0.2
Wall thickness of the upper chord member (Fig. 6(c))	4.2	4.7	10.6	0.17
Thickness of the C purline (Fig. 6(d))	2.5	3.0	16.7	0.17

Table 2 Comparison between the design load and the present load

Load classification	Design load (kN/m <sup>2</sup> )	Present load (kN/m <sup>2</sup> )
Permanent load	0.8	0.3
Variable load	0.5	0.5
Accumulated water load	0	0.3
Reference wind pressure	0.45	0.45

Table 3 Comparison between the static computation results before and after corrosion

Items	Before corrosion	After corrosion	Difference (%)
Maximum compressive stress (kN/m <sup>2</sup> )	175.5	174.2	0.7
Maximum tensile stress (kN/m <sup>2</sup> )	132.1	132.3	0.1
Maximum deformation value (mm)	29.0	32.0	10.3

corrosion rate of the steel truss has reached 10.6% and the cross section corrosion rate of the purline has reached 16.7%. The maximum corrosion speed rate of the components has reached 0.27 mm annually and the corrosion speed rate increased along with the wall thickness decreasing. Further, the present load values are estimated and compared with the design loads as shown in Table 2.

Then the static computation is performed on the structure using the design software – MSTCAD (LUO 2003). And the section dimensions are modified according to the actual corrosion results. For example the wall thickness of the upper chord in the steel tube truss which is 4.7 mm in design has been changed to 4.2 mm. However the computation load is same as the design load shown in Table 2. The boundary condition is the same as the drawings shown in Section 2. The calculated results are listed and compared with the results before corrosion in Table 3. Observing them we can get that the stress values satisfied the demand of the design code. On the other hand the maximum deformation value of the steel tube truss is 32 mm after corrosion. And it is less than the allowable value ( $l/250=23732/250=95$  mm) according to the code for design steel structures (GB 50017-2003). But the location of the maximum stress has changed before and after corrosion. This showed that the stress in the truss has redistributed.

Finally the strength and stiffness of the purlines are calculated based on the present section dimension (C160×70×20×2.5). The calculated maximum stress is 237 N/mm<sup>2</sup> which is larger than the design standard value (215 N/mm<sup>2</sup>). At the same time the maximum deformation value of purline has achieved 43.4 mm which is larger than the allowable value ( $l_0/200=6000/200=30$  mm). So the purlines in present have not satisfied the demand of the design code. They must be removed and changed to the new ones.

## 6. Analytical modal analysis

The finite element model of the whole structure as shown in Fig. 7 has been established by the finite element analysis package - ANSYS (1999). The finite element model included the triangle steel tube trusses, the declining lambdoid steel columns and the purlines. All element sections are tubular and the dimensions are same as the factual size. And the load is also same as the design load shown in Table 2. Three types of finite elements are used to model the different structural members. All the triangle steel tube trusses are modelled by the 3-D Spar elements (LINK 8). And the declining lambdoid steel columns and the purlines are modelled by the 3-D Elastic Beam elements (BEAM 4). The permanent load and the deadweight of the members are treated as lumped mass concentrated at the nodes of the tube truss and modelled by the Structural Mass elements (MASS 21). The material properties are taken from Q235BF steel where the elastic modulus is  $2.06 \times 10^{11}$  N/m<sup>2</sup> and the density is 7850 kg/m<sup>3</sup>. The modelling of the structural boundary conditions is an important issue in modal analysis. To simulate the actual cases as the description in Section 2, some efforts are made and implemented as follows: a) The x, z translational degrees of freedom and

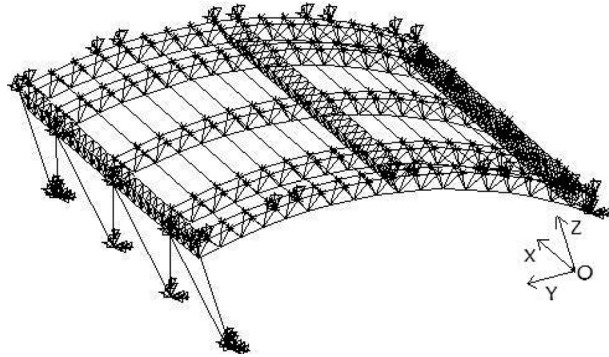
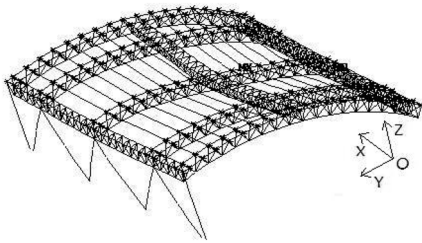
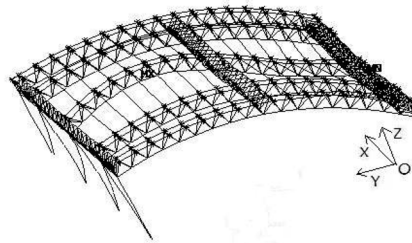


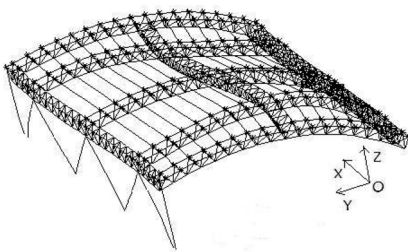
Fig. 7 Finite element model of the whole structure



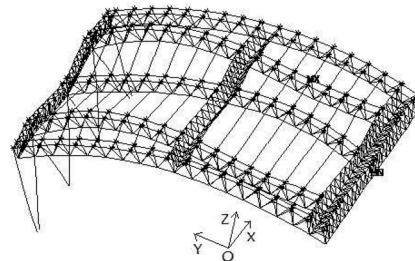
(a) The first mode shape



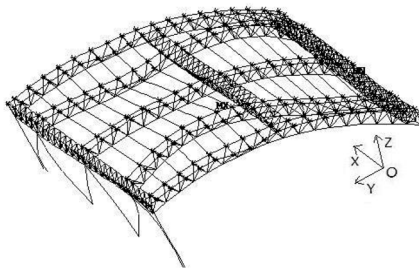
(b) The second mode shape



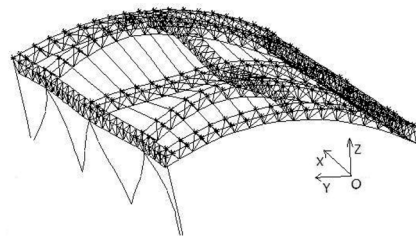
(c) The third mode shape



(d) The fourth mode shape



(e) The fifth mode shape



(f) The sixth mode shape

Fig. 8 Mode shapes of the whole structure calculated by finite element analysis

the y, z rotational degrees of freedom of the joints between the middle three tube trusses (HJ-2) and the declining steel columns are restrained; b) The x, y, z translational degrees of freedom and the x, z rotational degrees of freedom of the steel column bases are restrained; c) All the translational degrees of freedom and rotational degrees of freedom of the joints between the five tube trusses and the concrete columns are restrained; d) The x, z translational degrees of freedom of the bilateral tube trusses (HJ-1) are restrained on the nodes of the upper chord to simulate the influence of the glass wall on the bilateral tube truss.

Then the vibration properties were calculated by performing modal analysis based on the subspace iteration method. The structural dynamic characteristics including the first 6 natural frequencies and mode shapes are obtained and shown in Table 4 and Fig. 8. It is obvious that the structure has a narrow band of the low natural frequencies, which are close and coupled relatively. Observing the mode shapes, the fact can be get that mode shape 1 is the first vertical bending deflection of the whole roof, mode shape 2 is the second vertical bending deflection of the whole roof in the longitudinal direction, mode shape 3 is the second vertical bending deflection of the whole roof in the latitudinal direction, mode shape 4 behaves as a coupled vertical bending vibration between the middle three tube truss (HJ-2) and the horizontal connection truss (HJ-3~HJ-8), mode shape 5 behaves as a coupled second vertical bending vibration between the longitudinal direction and the latitudinal direction, mode shape 6 is the third vertical bending deflection of the whole roof in the latitudinal direction. In general the dynamic features of the structure are quite complex.

## **7. Field vibration test**

### *7.1 Measurement setup and data preprocessing*

Dynamic test on the natatorium can provide an accurate and reliable prediction of its global modal parameters including frequency, damping ratio and mode shape. And modal parameters are functions of the physical properties of the structure. The changes in the physical properties will cause changes in the modal properties. So, determining the modal properties of the structure through the full-scale vibration test is necessary to evaluate the structural performance. After field inspection, static computation and analytical modal analysis, the field vibration test on the whole structure were carried out. Firstly the locations of the acceleration sensors were optimized in order to identify the reliable modal parameters of the structure. This process is very important because that the arrangement result is extremely important for the modal test results. By considering the symmetry of the structure and the modal analysis results, 14 sensors were arranged in the direction of z axis and y axis. Fig. 9 gives the arrangement result of the measurement points on the natatorium. For example the number 7, 8, 13 sensors are located in the direction of y axis and others are located in the direction of z axis. The type of the acceleration sensor is CA-YD-132 which is produced in SINOCERA Piezotronics Inc. in P.R.CHINA. A 16-channel data acquisition system with signal amplifier and conditioner (Dynamic Signal Process System (DSPS)) which is produced in Beijing Aerospace Data Technology Company in P.R. CHINA is used to measure the vibration response for the modal test.

The natatorium is located in the middle of some tall buildings and the ambient vibrations induced by winds, traffic and pedestrians are not so visible. In order to obtain the abundant top-quality test data, the multiple-points random excitation method is taken as the excitation mode. The multiple-

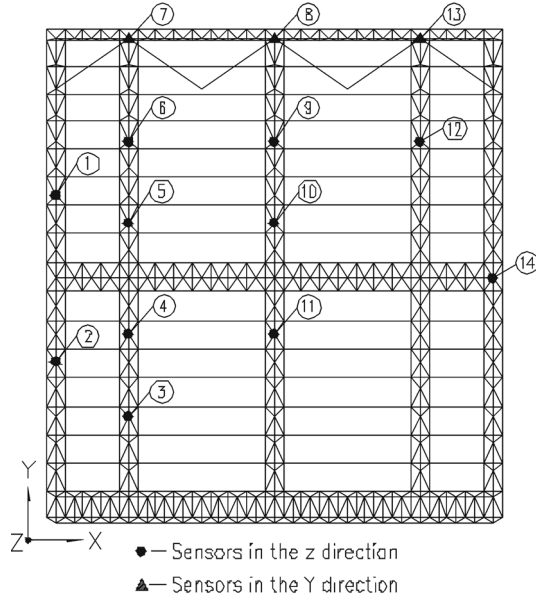


Fig. 9 Sensor arrangement for field vibration test

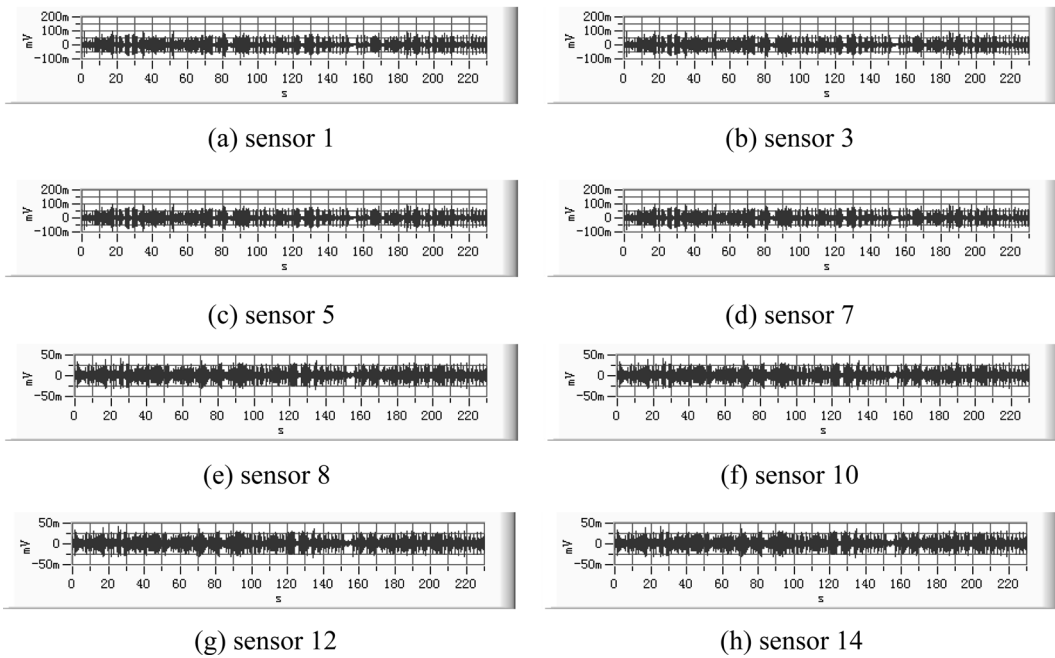


Fig. 10 Some typical time-domain signals in field vibration test

points random excitation method is an artificial means to simulate the ambient vibrations cases. The magnitude and the direction of the hammer forces are guaranteed to be random all through when several hammers beat the six declining steel columns (GZ in Fig. 1) synchronously. The later

research results showed that the substitute on the natural excitation is acceptable and feasible. The real time acquisition mode and the hard disk storage mode are adopted respectively in the process of data acquisition. The sampling frequency on site was 102.4 Hz, i.e., the analytical frequency is 40 Hz. At the same time the anti-aliasing filter had a cut-off frequency at 20 Hz. The data were simultaneously recorded for 230 seconds at all channels. As a result, totally 23552 data points were collected for each channel and there was 512 points data in each frame. Some typical time-domain signals of the measure points are shown as Fig. 10.

### 7.2 Operational modal analysis

Since the measured data are only response data, system identification methods using output-only responses are adopted to extract the modal information such as natural frequencies, mode shapes and damping ratios. This type of system identification is commonly called operational modal analysis. Two operational modal analysis methods are applied and evaluated in this study. They are Data-Driven Stochastic Subspace Identification (SSI-DATA) method (Overschee 1996), Frequency Domain Decomposition (FDD) / the Frequency-Spatial Domain Decomposition (FSDD) method (Brincker 2001, Zhang 2005, Wang 2005). And they are the time domain method and the frequency domain method respectively.

#### 7.2.1 SSI-DATA method

The Data-Driven Stochastic Subspace Identification (SSI-DATA) method directly utilizes the stochastic response data to identify the modal parameters. The identification process of SSI-DATA can be described as bellow: Firstly it estimates the state sequences directly from the given data through an orthogonal or oblique projection of the row spaces of the future outputs into the row spaces of the past outputs. Secondly the singular value decomposition (SVD) is performed to determine the system order, the observability matrix and the Kalman state sequence. Then the state

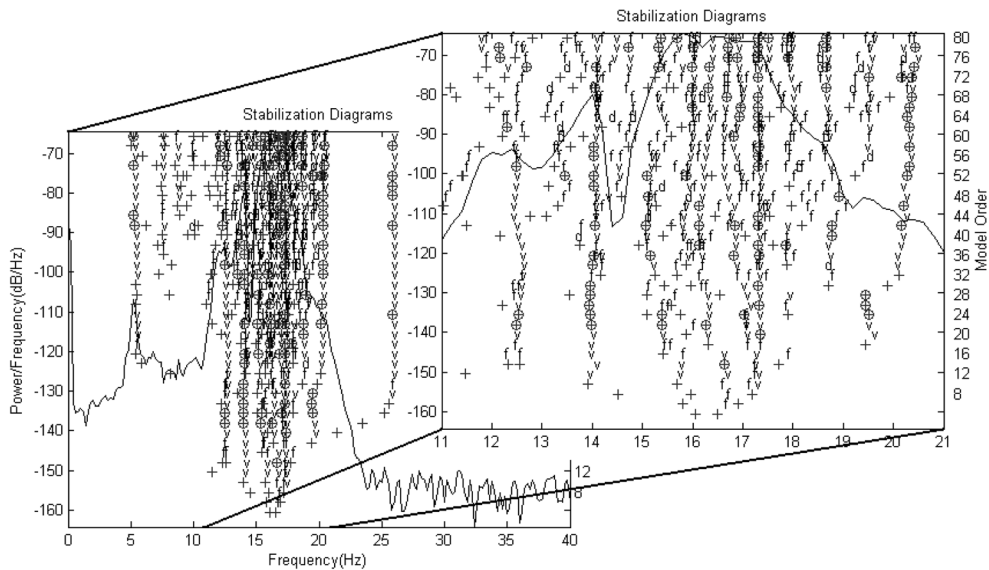


Fig. 11 Stability diagram obtained by SSI-DATA algorithm

space model is extracted through the solution of a least squares problem. Finally the modal parameters including natural frequencies, damping ratios and mode shapes can be obtained by eigenvalue decomposition acting on the state space model matrix. For more detail readers could refer to the exhaustive presentation in literature (Overschee 1996).

When the SSI-DATA method is implemented, the Canonical Variant Analysis (CVA) algorithm is adopted (Overschee 1996). In operation of SSI-DATA method, all 23552 samples  $\times$  14 channels of one setup were treated once. Consecutive state space models of order 2 to 80 in steps of 2 were identified. From all these state space models, the modal parameters are extracted and plotted in a stabilization diagram as shown in Fig. 11. The background curve is the sum of all the auto- and cross-spectral density functions which are obtained by selecting the sensor 5 as the reference point. The used symbols are: “ $\oplus$ ” for a stable pole; “v” for a pole with stable frequency and modal vector; “d” for a pole with stable frequency and damping; “f” for a pole with stable frequency and “+” for a new pole. The stabilisation criteria are: 1% for frequencies, 5% for damping ratio and 5% for mode shapes.

### 7.2.2 FDD/FSDD method

The Frequency-Spatial Domain Decomposition (FSDD) method (Zhang 2005, Wang 2005) is presented as an extended version of the Frequency Domain Decomposition (FDD) method (Brincker 2001). They all belong to the frequency or frequency and spatial domain methods. In FDD method, the first step is to estimate the power spectral density (PSD) matrix from the measurements and then it is decomposed at each frequency line by taking the singular value decomposition (SVD) technique. When the frequency approaches to a modal frequency the mode shape is dominating there. Then the first singular vector is an estimation of the mode shape. Meanwhile the corresponding singular value is the auto power spectral density function of the corresponding single degree of freedom system. So the natural frequencies can be located at the peaks from the singular

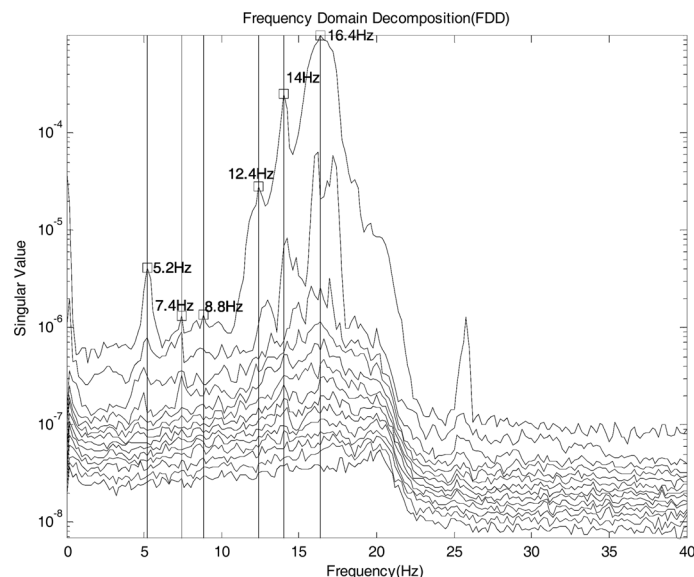


Fig. 12 Six natural frequencies identified by FDD algorithm

value plot. Further investigation on these methods, Zhang (2005) and Wang (2005) presented the FSDD method in which the concept of enhanced output PSD is proposed via pre-multiplying and post-multiplying a singular vector corresponding to the damped natural frequency. It suggests that any curve fitting algorithm based on single degree of freedom (SDOF) can be used to estimate the modal frequency and damping ratio (Zhang 2005). The reason is that the enhanced PSD can be taken as Frequency Response Function (FRF) of a single degree of freedom (SDOF) system in the vicinity of the modal frequency. In the other hand, Wang (2005) applied the least square technique on the enhanced PSD function to obtain the pole and further the modal frequency and damping ratio.

For the FDD/FSDD method, 46 segments of 512 data points were transformed to the frequency domain. The Hanning window, 50% overlap of each segment and the time domain average technique are implemented to estimate the power spectral densities. The identified six natural frequencies, i.e., the picked peak of the singular values of the spectral density matrices by FDD algorithm is shown in Fig. 12. The last two are the higher natural frequencies. Obviously the estimation accuracy of the natural frequencies by FDD is limited by the frequency resolution. To increase the estimation accuracy, the FSDD algorithm is further implemented and the enhanced PSD is obtained first. Then the least square algorithm is applied to the enhanced PSD function to obtain this pole and the accurate modal frequency and damping ratio were estimated.

### 7.3 Comparison of modal results

In this section, the identification results of the two methods are presented and compared. Table 4

Table 4 Comparison of natural frequencies obtained by the two methods and FEM (Hz)

No.	FEM	SSI-DATA		FDD/FSDD	
	Freq.	Freq.	Discrepancy (%)	Freq.	Discrepancy (%)
1	6.3306	5.1954	-17.93	5.2436	-17.17
2	7.9865	7.4290	-6.98	7.3763	-7.64
3	8.3295	8.5411	2.54	8.6719	4.11
4	9.182	----	----	----	----
5	9.474	----	----	----	----
6	10.096	12.576	24.56	12.925	28.02

Table 5 Comparison of damping ratios obtained by the two methods

No.	Damping Ratio (%)	
	SSI-DATA	FDD/FSDD
1	4.74	4.83
2	3.70	----
3	6.99	3.18
4	----	----
5	----	----
6	3.05	8.69

and Table 5 are the comparison results of natural frequencies and damping ratios respectively. All the two methods can only identify four natural frequencies which are the first, second, third and sixth natural frequencies. It is regretful that the fourth and fifth natural frequencies are not identified. The reason potentially is that the fourth and fifth natural frequencies are close and coupled badly. Further these results are compared with the analytical results obtained from the finite element method. It is obvious that these identification techniques are satisfied and the discrepancy can be accepted in the engineering. And the first two natural frequencies identified are all lower than the calculated ones by FEM. This may be because the natorium structure is suffering some accumulated damage such as corrosion, crack and delamination on some main components. Table 5 also shows that the damping ratios can all be estimated by the two methods. The first damping ratios identified by SSI-DATA and FDD/FSD are 4.74% and 4.83% respectively. They are close to the stated value 5% of the steel structure as shown in Code for seismic design of buildings (GB 50011-2001) in China. That means that these estimations are reliable.

From Fig. 13 to Fig. 14, the mode shapes determined by the two identification methods are shown respectively. The mode shape data in the nodes which is not arranged the sensors are acquired according to the symmetry of the structure and the analytical modal analysis results. Comparing them with the calculated mode shapes by analytical modal analysis as shown in Fig. 8, the identified mode shapes are very close to the numerical results. As they appeared, the whole steel truss was provided with the vibration characteristic of the column shell under the action of the purlines. That means that they are all consistent with the mode shapes calculated by FEM respectively.

To further demonstrate the effectiveness of the two different identification methods, the Modal Assurance Criterion (MAC) values between the corresponding mode shapes of the two identification algorithms and FEM are calculated and plotted respectively in Fig. 15 to Fig. 17. It is obvious that the mode shapes identified by the two methods are quite good agreement each

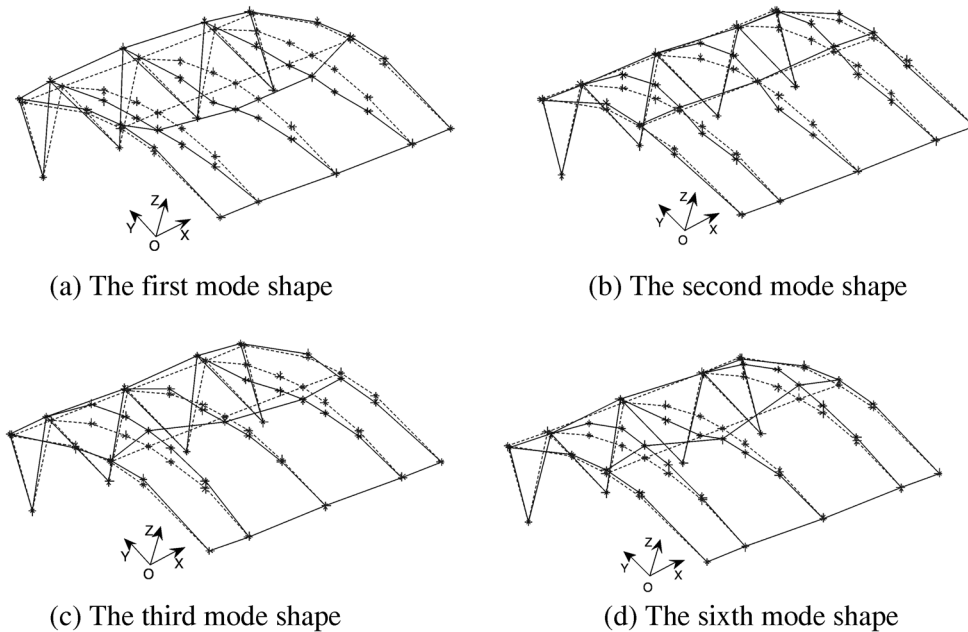


Fig. 13 Identified mode shapes by SSI-DATA algorithm

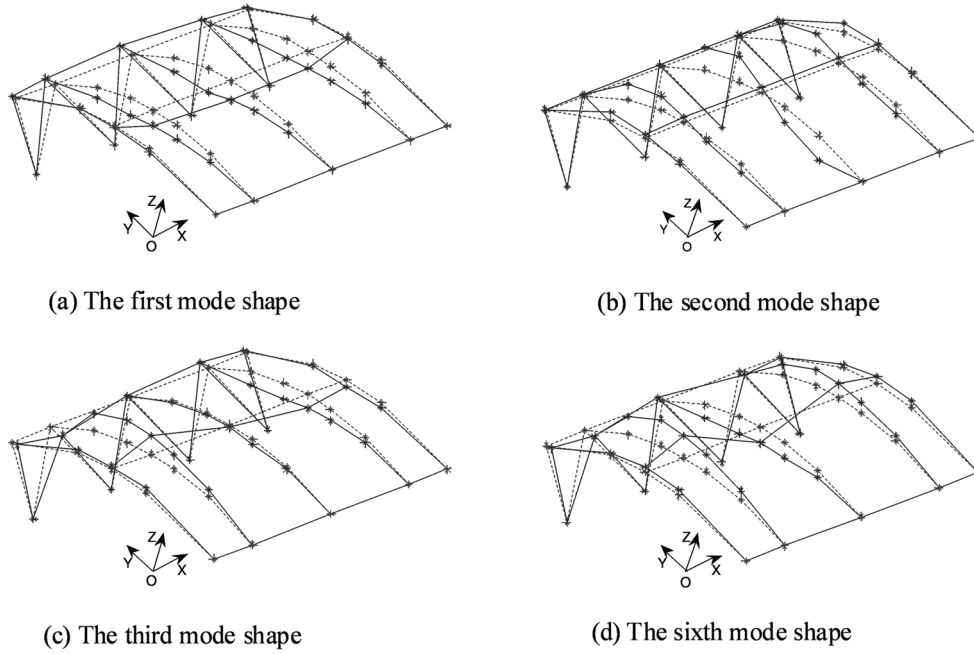


Fig. 14 Identified mode shapes by FDD/FSDD algorithm

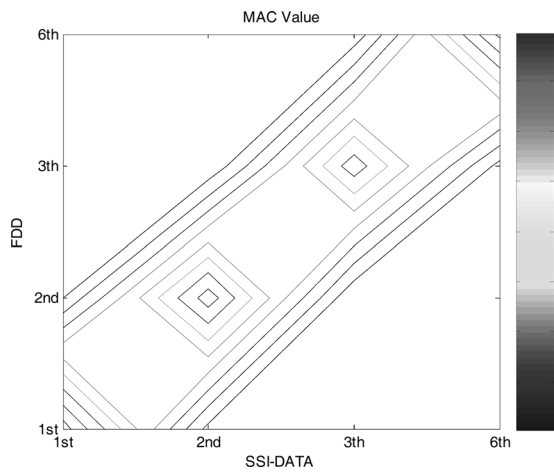


Fig. 15 MAC-values between FDD/FSDD and SSI-DATA

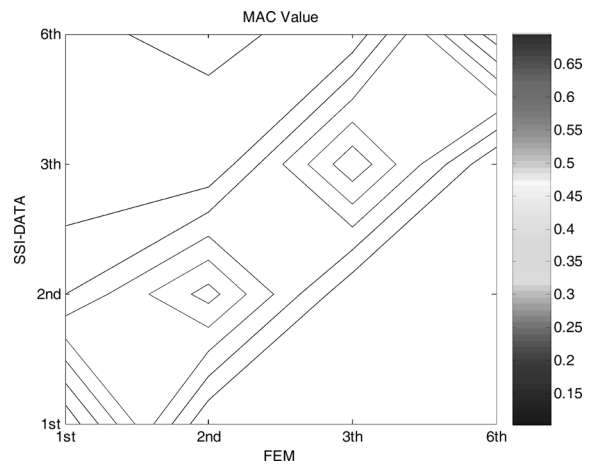


Fig. 16 MAC-values between FEM and SSI-DATA

other. And the mode shapes identified are comparatively good agreement with the FEM results. In order to quantify this agreement, the mode shapes calculated by finite element analysis is replotted in the compact form as shown in Fig. 18. Obviously the results are good agreement with the experimental results shown in Fig. 13 and Fig. 14. So we can further conclude that the identified mode shapes are reliable.

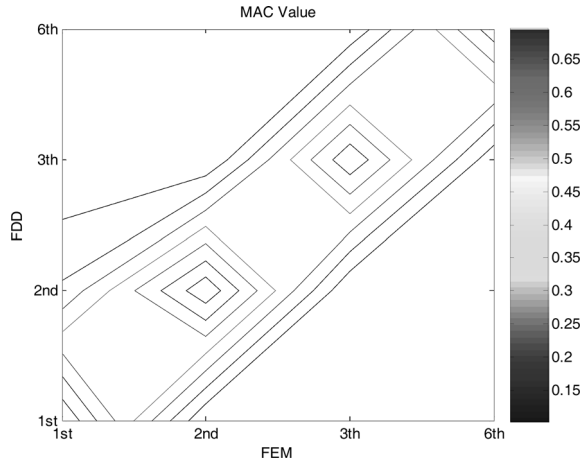


Fig. 17 MAC-values between FEM and FDD/FSDD

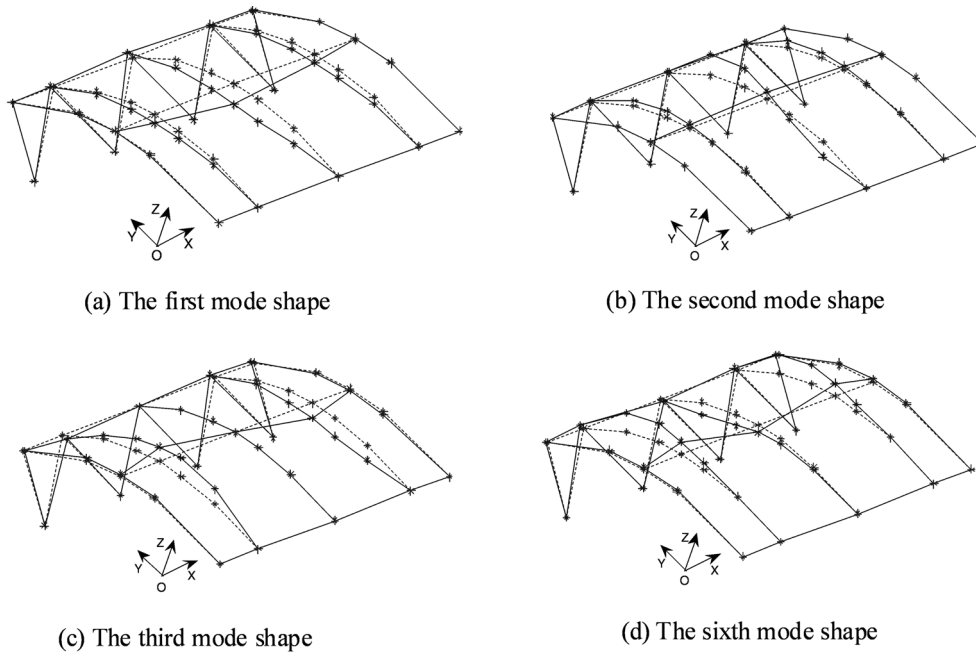


Fig. 18 Calculated mode shapes by FEM

**8. Conclusions**

This paper has presented a systematic procedure on structural evaluation of an existing steel natatorium in service by FEM and dynamic measurement. The procedure is based on the experimental and numerical methods synthetically. The following conclusions and suggestions are drawn from the study:

- 1) Through the intuitionistic observation, the corrosion and rust-eaten results of the whole

natatorium are serious. The work of cleaning rust and corrosion must be done on the triangle steel tube trusses, the declining lambdoid steel columns and the column bases according to the correlative national codes in China. The cable which hung the glass curtain wall must be tensioned over again. Further the maintenance work on the above components must be done periodically in the future.

- 2) The leak tightness of the colour interlayer steel plate is not so good that the indoor vapour and the outdoor rainwater have intruded in the heat preservation layer of the roof system, i.e. the thick rock wool. This caused that the heat preservation layer is disabled, the purlines are corroded and the accumulated water is overloaded. So the design on the detail conformation of the roof nodes must be considered carefully in the similar engineering design. The detail conformation may include the connection between the bracket of the upper chord and the colour interlayer steel plate, the connection between the colour interlayer steel plate and the lateral glass curtain wall.
- 3) Through the field inspection and the static computation, the strength and stiffness of the triangle steel tube truss in its actual status can still satisfy the demand of the code for design steel structures (GB 50017-2003) in China. But the location of the maximum stress has changed before and after corrosion. And because of the above overweighted accumulated water load, the strength and stiffness of the purlines in present have not satisfied the demand of the code for design steel structures (GB 50017-2003) in China. They must be removed and redesigned entirely. At the same time the skeleton which hung on the drop ceiling also must be taken down and rebuilt completely.
- 4) To evaluate the structural performance of the natatorium, the dynamic properties including modal frequencies, mode shapes and damping ratios are used and identified by two different system identification methods through the field vibration test. The two system identification methods are the SSI-DATA method and the FDD/FSDD method. They showed their efficiency in identifying the close mode shapes. And it is necessary to use different identification techniques because they can verify each other and increase the reliability of the identified results.
- 5) The analytical modal analysis and field vibration test provides a comprehensive investigation of the dynamic properties of the natatorium. The dynamic response of the natatorium is characterized by the presence of many closely spaced, coupled modes. As the action of the purlines and roof system the whole natatorium provided the vibration characteristic of the column shell. The analytical and the experimental modal frequencies and mode shapes are all correlative and consistent quite well each other by comparing the MAC values.
- 6) In implementation of SSI-DATA, the problems with model order determination and structural modes distinguishing become much more significant in operational modal identification. In this paper the stabilization diagram which is a graphical approach is constructed and used to select the true modes after realization of modal parameters. This procedure facilitates the selection of genuine modes from computational or fictitious modes. In FDD/FSDD method the accuracy of the estimated modal frequencies is limited to the estimation of the PSD spectrum, such as measurement noise and leakage error. So the window function and the time domain averaging technique should be employed in FFT calculation and the length of data also should be increased by all means.

## Acknowledgements

This research is financially supported by the National Science Foundation of China under the grant number 50478030 and the Key Technologies Research and Development Program of Heilongjiang Province in China under the grant number GC04C101.

## References

- Abdel-Ghaffar, A.M. and Scanlan, R.H. (1985), "Ambient vibration studies of Golden Gate bridge, I: Suspended structure", *J. Eng. Mech.*, **111**(4), 463-482.
- ANSYS®. (1999), *User's Manual, Revision 5.6*. USA: Swanson Analysis System.
- Brincker, R., Zhang, L.M. and Anderson, P. (2001), "Modal identification of output-only systems using frequency domain decomposition", *Smart Mater. Struct.*, **10**(3), 441-445.
- Cunha, A., Caetano, E. and Delgado, R. (2001), "Dynamic tests on large cable-stayed bridge", *J. Bridge Eng.*, **6**(1), 54-62.
- Galvin, P. and Dominguez, J. (2007), "Dynamic analysis of a cable-stayed deck steel arch bridge", *J. Constr. Steel Res.*, **63**(8), 1024-1035.
- Gentile, C. and Saisi, A. (2007), "Ambient vibration testing of historic masonry towers for structural identification and damage assessment", *Constr. Build. Mater.*, **21**(6), 1311-1321.
- Hai, D.T. (2006), "Current status of existing railway bridges in Vietnam: an overview of steel deficiencies", *J. Constr. Steel Res.*, **62**(10), 987-994.
- Jaishi, B., Ren, W.X., Zong, Z.H. and Maskey, P.N. (2003), "Dynamic and seismic performance of old multi-tiered temples in Nepal", *Eng. Struct.*, **25**(14), 1827-1839.
- Luo, Y.Z. (2003), *MSTCAD Instruction Manual*. Space Structures Research Center of Zhejiang University. (in Chinese)
- Magalhaes, F., Caetano, E. and Cunha, A. (2008), "Operational modal analysis and finite element model correlation of the Braga Stadium suspended roof", *Eng. Struct.*, **30**(6), 1688-1698.
- McCrea, A., Chamberlain, D. and Navon, R. (2002), "Automated inspection and restoration of steel bridges - a critical review of methods and enabling technologies", *Automat. Constr.*, **11**(4), 351-373.
- Melchers, R.E. (2005), "The effect of corrosion on the structural reliability of steel offshore structures", *Corrosion Science*, **47**(10), 2391-2410.
- Onoufriou, T. and Frangopol, D.M. (2002), "Reliability-based inspection optimization of complex structures: A brief retrospective", *Comput. Struct.*, **80**(12), 1133-1144.
- Ren, W.X., Peng, X.L. and Lin, Y.Q. (2005), "Experimental and analytical studies on dynamic characteristics of a large span cable-stayed bridge", *Eng. Struct.*, **27**(1), 535-548.
- Siringoringo, D.M. and Fujino, Y. (2008), "System identification of suspension bridge from ambient vibration response", *Eng. Struct.*, **30**(1), 462-477.
- Van Overschee, P. and De Moor, B. (1996), *Subspace Identification for Linear Systems - Theory Implementation Applications*, Kluwer Academic Publishers, Dordrecht (Netherlands).
- Wang, T., Zhang, L.M. and Tamura, Y. (2005), "An operational modal analysis methods in frequency and spatial domain", *Earthq. Eng. Eng. Vib.*, **4**(2), 295-300.
- Wenzel, H. and Pichler, D. (2001). *Ambient Vibration Monitoring*. John Wiley & Sons, Ltd. New York.
- Zhang, L.M., Brincker, R. and Andersen, P. (2005), "An overview of operational modal analysis: Major development and issues", *Proceedings of the 1st International Operational Modal Analysis Conference*, Copenhagen, Denmark, 179-190.
- Zhang, L.M., Wang, T. and Tamura, Y. (2005), "A Frequency-spatial domain decomposition (FSDD) technique for operational modal analysis", *Proceeding of the 1st International Operational Modal Analysis Conference*, Copenhagen, Denmark, 551-561.